IEEE Access
Multidisciplinary | Rapid Review | Open Access Journal

Received September 7, 2021, accepted September 14, 2021, date of publication September 23, 2021,
date of current version December 10, 2021.

Digital Object Identifier 10.1109/ACCESS.2021.3115164

Global-Equivalent Sliding Mode Control Method for Bridge Crane

TIANLEI WANG[1,2], (Member, IEEE), NANLIN TAN[1], JIONGZHI QIU[2], YANJIANG YU[3], XIANWEN ZHANG[1,2], YIKUI ZHAI[2,4], (Member, IEEE), RUGGERO DONIDA LABATI[4], (Member, IEEE), VINCENZO PIURI[4], (Fellow, IEEE), AND FABIO SCOTTI[4], (Senior Member, IEEE)

[1]School of Mechanical, Electronic and Control Engineering, Beijing Jiaotong University, Beijing 100044, China
[2]Department of Intelligent Manufacturing, Wuyi University, Jiangmen 529020, China
[3]School of Mechanical and Automotive Engineering, South China University of Technology, Guangzhou 510640, China
[4]Departimento di Information, Universita degli Studi di Milano, 20133 Milano, Italy

Corresponding author: Tianlei Wang (tianlei.wangi@aliyun.com)

This work was supported in part by the National Natural Science Foundation of China under Grant 51505154 and Grant 51437005; in part by the Science and Technology Project of Jiangmen City under Grant 2020JC01035 and Grant 2020JC01016; and in part by the College Students' Innovative Entrepreneurial Training Plan Program under Grant S202011349041, Grant 202011349028, and Grant 202011349296.

ABSTRACT A wide application of sliding mode variable structure control as a nonlinear robust control method, has been witnessed in anti-swing positioning control of bridge crane system. Aiming at the problem that the sliding mode variable structure control system of bridge crane is not robust in approaching process, a new Global-Equivalent Sliding Mode Controller (GESMC) based on bridge crane system is proposed. This controller can realize the anti-sway positioning control of the bridge crane system under the condition of uncertain model parameters and external disturbance. The proposed controller, different from the traditional sliding mode control, excels in improving system robustness through keeping the system states in the sliding surface during the whole response process. Specifically, it initiates with the design of a global sliding surface, which can eliminate the sliding mode approach process of the system and achieve global robustness in the system. Afterwards, a new switching function combined with the equivalent sliding mode control method is incorporated to effectively reduce the chattering generated when the system reaches the sliding mode manifold. Its asymptotic stability is proven without a priori knowledge on the bounds of unknown disturbances by using the Lyapunov stability theory. Lastly, the simulation conducted verifies the effectiveness and robustness of the GESMC proposed in this paper and meanwhile demonstrates a comparatively favorable performance for the GESMC in reducing chattering.

INDEX TERMS Bridge crane, anti-swing positioning control, global-equivalent sliding mode control, global robustness, chattering.

I. INTRODUCTION

Bridge-type cranes act an indispensable role in modern logistics such as ports, warehouses, construction sites and so on. However, as a typical nonlinear undereducated system, bridge-type crane system features with multivariable and strong coupling, which gives rise to challenges in designing a high performance controller for crane systems to realize the anti-swing positioning control.

The associate editor coordinating the review of this manuscript and approving it for publication was Shihong Ding.

Many control schemes have been presented for bridge cranes in the past decades, which can be roughly categorized as open-loop control and closed loop-control. Representative methods of open-loop control include optimal control [1], [2], trajectory planning [3], [4] and input shaping control [5], [6], yet whose strong dependence and low robustness hinder their application in real-world practices. For this reason, a series of closed-loop control methods have been suggested by numerous scholars, including dynamic PID control [7], fuzzy PID control [8], adaptive neural network control [9], etc.

Sliding mode variable structure control is a nonlinear closed-loop control method with strong robustness,

which has been extensively used in bridge crane systems in recent years, such as Conventional Sliding Mode Control (CSMC) [10], [11], Hierarchical Sliding Mode Control (HSMC)[12]–[14], Terminal Sliding Mode Control [15]–[17], decoupled Sliding Mode Control [18], [19], adaptive Sliding Mode Control [20]–[22], fuzzy Sliding Mode Control [23], [24], etc. The proposal of sliding mode variable structure control facilitates precise positioning and anti-swing control of the bridge crane system. Nevertheless, because of the long approach time in the sliding mode control method above, strong robustness only exists in the sliding mode switching stage but in the approach process, which means that it only possesses local robustness. In this regard, some scholars have conducted improvements on the traditional sliding mode. Specifically, a time-varying ellipsoid sliding mode control method was designed in [25]. By adjusting the vertical radius of the ellipsoid sliding surface, the system states can quickly approach the sliding mode manifold and effectively improve the smoothness and robustness. Cui and Xu [26] introduced a new adaptive sliding mode control method based on considering the time-varying delay and processing disturbance of the system, which can guarantee the attraction of the sliding mode to the first-order sliding mode surface in certain amount of time. In [27], Lu *et al.* introduced a time-varying sliding enhanced anti-control scheme by designing a piecewise-defined time function including trigonometric functions, which not only eliminated the arrival phase of tracking error, but also ensured the finite-time convergence of the tracking error. However, although the proposed controller can effectively shorten the approach time of the system states to the sliding mode surface by designing the nonlinear time-varying sliding mode surface, it still cannot solve the defect of weak anti-disturbance ability in the approach process of the system. So it can only ensure the local robust control of the system during the control process.

In this paper, a new sliding mode controller with global convergence effect is introduced for two-dimensional bridge crane to overcome the local robustness defect of traditional sliding mode controller. Firstly, the dynamic model of the bridge crane with friction and air resistance considered is established, therefore constructing a new type of whole sliding surface. Afterwards, a nonlinear controller is devised with the equivalent sliding mode controller, which features with high robustness against parameter variations, external disturbances and other uncertain model factors. What's more, the analysis of Lyapunov stability theory can certify the asymptotic stability of the system. Lastly, so as to verify the potency of the proposed GESMC, simulation and verification by MATLAB/Simulink platform on the proposed GESMC are conducted with comparison to CSMC controller and PID controller based on the approach law. Simulation results are presented to verify the superior performance of GESMC. The advantages of the controller proposed in this paper are as follows:

1) A global equivalent sliding mode control method is proposed, which can skip the sliding mode approach process, overcomes the shortcomings of traditional sliding mode control in the approach stage, and makes the controller have global robust control performance.
2) It owns better control effect under the condition of the model parameters change, which is validated by simulation results.
3) Due to the specific design of the switching function, the control input is essentially continuous, avoiding chattering problems and potential damage to the actuating devices.

The rest of this paper is organized as follows. In Section II, the dynamic model of two-dimensional bridge crane is briefly introduced and the control problem is formulated. In Section III, the main results, including the GESMC law develop and stability analysis of the closed-loop system, are given. To verify the superior performance of the proposed method, some numerical simulations are provided in Section IV. Section V gives conclusions.

II. MATHEMATICAL MODEL OF TWO-DIMENSIONAL BRIDGE CRANE

The two-dimensional bridge crane used in this paper is an underactuated system with two inputs, three outputs and 3 degrees of freedom shown in Fig. 1. Table 1 can be referred to the parameters of the two-dimensional bridge crane system in the figure.

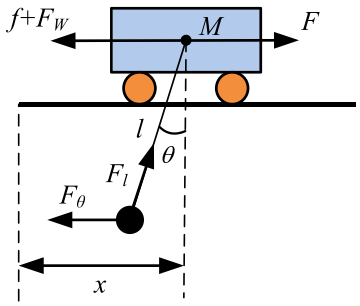

FIGURE 1. Physical model of bridge crane.

TABLE 1. Model parameters of bridge crane system title.

Symbol	Physical quantity	Symbol	Physical quantity
M	The mass of the crane	F	Horizontal driving force of crane
m	Mass of Payload	F_w	Air resistance to the crane
f	Friction between crane and track	F_θ	Air resistance to payload
μ	Friction coefficient between crane and track	F_l	Lift of wire rope
x	Horizontal displacement of crane	a_1	Windward area of crane

In this paper we make the following assumptions about the above model to facilitate our subsequent analysis.

Hypothesis 1: Both the crane and the payload are objects with uniform mass distribution and can be regarded as known particles.

Hypothesis 2: The mass and elastic deformation of the wire rope are ignored in this model.

Hypothesis 3: The swing Angle θ ranges in: $-\pi/2 < \theta(t) < \pi/2$;

Hypothesis 4: The presence of the first and second derivatives of x_d, θ_d and l_d is ensured, and x_d and l_d are not accepted as zero during the whole control process;

For the two-dimensional bridge crane with variable rope length as shown in Fig. 1, its dynamic characteristics can be described by the following model:

$$(M+m)\ddot{x} - ml\cos\theta\ddot{\theta} - m\sin\theta\ddot{l} - 2m\dot{l}\dot{\theta}\cos\theta - ml\dot{\theta}^2\sin\theta = F - f - F_w \tag{1}$$

$$-ml\cos\theta\ddot{x} + ml^2\ddot{\theta} + 2ml\dot{l}\dot{\theta} + mgl\sin\theta = -F_\theta \tag{2}$$

$$-m\sin\theta\ddot{x} + m\ddot{l} - ml\dot{\theta}^2 - mgl\sin\theta = F_l \tag{3}$$

In engineering practice, bridge crane can often be spotted in port cargo loading and unloading. Thus, the friction and air resistance caused by rust and wind resistance cannot be ignored because of the wet and strong wind marine environment. The following linear model of friction force takes the air resistance of the system and the friction between the crane and the track into account during its establishment:

$$f = \mu\dot{x} \tag{4}$$

where μ represents the friction coefficient between the crane and the track. In terms of air resistance, this paper adopts an air resistance model of bridge crane at low speed, which considers the moving speed of the object, the density of the air and the geometric shape of the object. Its expression shows as follows:

$$\begin{cases} F_w = ka_1\dot{x}^2 + ka_2(\dot{x} - \dot{l}\sin\theta - l\dot{\theta}\cos\theta)^2 \\ F_\theta = ka_2\left[l(\dot{x} - \dot{l}\sin\theta - l\dot{\theta}\cos\theta)\cos\theta\right]^2 \end{cases} \tag{5}$$

In the formula, k refers to the air resistance coefficient considering air density while a_1 and a_2 represent the windward cross-sectional areas of the crane and the payload respectively. By combining (2), (3), (4), (5) and (6), the state space model of two-dimensional bridge crane system can be worked out as:

$$\dot{\boldsymbol{X}}_1 = \boldsymbol{X}_2, \tag{6}$$

$$\dot{\boldsymbol{X}}_2 = \boldsymbol{A}(\boldsymbol{X}_1, \boldsymbol{X}_2) + \boldsymbol{B}(\boldsymbol{X}_1, \boldsymbol{X}_2)\boldsymbol{U} + L(\boldsymbol{X}_1)\boldsymbol{F}_d. \tag{7}$$

where $\boldsymbol{X_1} = [x, \theta, l]^{\mathrm{T}}$, $\boldsymbol{U}$=$[F, 0, F_l]^{\mathrm{T}}$, $\boldsymbol{F}_d$ =$[f + F_w, F_\theta, 0]^{\mathrm{T}}$ represent state vector, input and damping force vector, separately. And $\boldsymbol{A}(\boldsymbol{X}_1, \boldsymbol{X}_2)$, $\boldsymbol{B}(\boldsymbol{X}_1, \boldsymbol{X}_2)$ and $\boldsymbol{L}(\boldsymbol{X}_1)$ are defined as, shown at the bottom of the page.

To sum up, this paper intends to design a controller with global robustness which is applicable to the nonlinear system, so that the bridge crane system can reduce the value of swing angle θ as much as possible while ensuring the rapid reach of x and l at the target values.

III. CONTROLLER DESIGN AND STABILITY ANALYSIS

As a variable structure controller based on the whole equivalent sliding mode control, the controller of the bridge crane system proposed in this paper is designed with the construction of sliding mode surface followed by control law design.

A. SLIDING SURFACE CONSTRUCTION

In order to achieve the global robustness of the controller, this paper adopts a global sliding mode surface with global convergence performance. Meanwhile, since the bridge crane system is a typical underactuated system, and the swing angle is an underactuated quantity in the system, we can get the following equation (8) by dividing both sides of Formula (2) by ml:

$$-\cos\theta\ddot{x} + l\ddot{\theta} + 2\dot{l}\dot{\theta} + g\sin\theta = -\frac{F_\theta}{ml} \tag{8}$$

Equation (8) describes the coupling relationship between payload swing and trolley movement, indicating that crane displacement plays a significant role in effectively suppressing and eliminating residual payload swing. For this reason, the following global sliding surface of the crane position change and the global sliding surface of the rope length

$$\boldsymbol{A}(\boldsymbol{X}_1, \boldsymbol{X}_2) = \begin{bmatrix} \dfrac{glm - glm\cos^2\theta + 2\dot{\theta}^2 lm\sin\theta - gm\cos\theta\sin\theta}{M} \\ \dfrac{\dot{\theta}^2 lm\sin(2\theta) + glm\cos\theta - glm\cos^3\theta - gm(\sin\theta - \sin^3\theta) - 2M\dot{l}\dot{\theta} - Mg\sin\theta}{Ml} \\ \dfrac{2\dot{\theta}^2 lm + gm\cos^3\theta + glm\sin\theta + M\dot{\theta}^2 l - gm\cos\theta - 2\dot{\theta}^2 lm\cos^2\theta + Mgl\sin\theta - glm\cos^2\theta\sin\theta}{M} \end{bmatrix}$$

$$\boldsymbol{B}(\boldsymbol{X}_1, \boldsymbol{X}_2) = \begin{bmatrix} \dfrac{1}{M} & 0 & \dfrac{\sin\theta}{M} \\ \dfrac{\cos\theta}{Ml} & 0 & \dfrac{\sin 2\theta}{2Ml} \\ \dfrac{sin\theta}{M} & 0 & \dfrac{M + m - m\cos^2\theta}{Mm} \end{bmatrix}, \quad \boldsymbol{L}(\boldsymbol{X}_1) = \begin{bmatrix} -\dfrac{1}{M} & -\dfrac{\cos\theta}{Ml} & 0 \\ -\dfrac{\cos\theta}{Ml} & -\dfrac{M + m\cos^2\theta}{Ml^2 m} & 0 \\ -\dfrac{sin\theta}{M} & -\dfrac{cos\theta sin\theta}{Ml} & 0 \end{bmatrix}$$

change with dynamic swing Angle are designed as:

$$\begin{cases} s_x = \dot{e} + c_1 e + c_2 \theta - f_1(t) \\ s_l = \dot{e}_l + c_3 e_l - f_2(t) \end{cases} \tag{9}$$

in which c_1, c_2 and c_3 are normal numbers more than zero; e represents the deviation of position x; e_l denotes the deviation of rope length l; $f_1(t)$ and $f_2(t)$ are the initial functions of the above two whole sliding mode surfaces, which can be expressed as:

$$\begin{cases} e = x - x_d \\ e_l = l - l_d \\ f_1(t) = (e_0 + c_1 e_0)\mathrm{e}^{-k_1 t} = -c_1 x_d \mathrm{e}^{-k_1 t} \\ f_2(t) = c_3(l_0 - l_d)\mathrm{e}^{-k_2 t} \end{cases} \tag{10}$$

where k_1 and k_2 are constants greater than zero. The variable structure sliding mode control system operates with the entry from the initial point and then stays in the sliding mode driven by control law. Under the guidance of the sliding mode movement, the system approaches the origin of the phase plane (i.e. the system equilibrium point).

Obviously, according to Equations (8) and (9), when $x = 0$, $\theta = 0$, $s_x(t) = 0$, and when $l = 0$, $s_l(t) = 0$, that is, the system trajectory will land on the switching plane from the beginning, avoiding the interference of the external environment in the dynamic sliding mode approaching stage of the system, which certified the global robustness of the system.

B. CONTROL LAW DESIGN

This paper adopts the equivalent sliding mode controller design method and establishes a continuous smooth switching function to undermine the chattering effect. This design method will be expounded in the following paragraphs. First, let the change law of sliding mode surface be 0, which means:

$$\boldsymbol{\Omega}\left[\boldsymbol{A}(\boldsymbol{X}_1, \boldsymbol{X}_2) + \boldsymbol{B}(\boldsymbol{X}_1, \boldsymbol{X}_2)\boldsymbol{U_{eq}} + \boldsymbol{L}(\boldsymbol{X}_1)\boldsymbol{F}_d\right] + \boldsymbol{\Phi}(\boldsymbol{X}_1, \boldsymbol{X}_2) = 0 \tag{11}$$

Including $\boldsymbol{U_{eq}} = [F_{eq},\ 0,\ F_{leq}]^{\mathrm{T}}$ equivalent control, the control system of F_{eq} and F_{leq} crane horizontal driving force F respectively and wire rope lift F_l in their respective sliding mode surface $s_x(t)$ and $s_l(t)$ on the equivalent control term, $\Omega \in \mathbb{R}^{3\times3}$, $\Phi \in \mathbb{R}^{3\times1}$ as the auxiliary matrix, defined as:

$$\boldsymbol{\Omega} = \begin{bmatrix} 1 & 0 & 0 \\ 0 & 0 & 0 \\ 0 & 0 & 1 \end{bmatrix}, \quad \boldsymbol{\Phi}(\boldsymbol{X}_1, \boldsymbol{X}_2) = \begin{bmatrix} c_1\dot{x} + c_2\dot{\theta} - \dot{f}_1(t) \\ 0 \\ c_3\dot{l} - \dot{f}_2(t) \end{bmatrix}$$

Hence, the equivalent control quantity of the controller can be defined as (12), shown at the bottom of the page.

For the dynamic system of the bridge crane shown in Equations (1)∼(3), the control law designed in this paper is:

$$\begin{cases} F = F_{eq} + F_{sw} \\ F_l = F_{leq} + F_{lsw} \end{cases} \tag{13}$$

where F_{sw} and F_{lsw} refer to the switching robust terms of the horizontal driving force F of the crane and the lifting force F_l of the wire rope on the sliding surface $s_x(t)$ and $s_l(t)$ respectively which can be obtained through setting $\dot{S}_x = -K_1 s_x - \eta_1 \mathrm{sgn}(s_x)$ and $\dot{s}_l = -K_2 s_l - \eta_2 \mathrm{sgn}(s_l)$ [10], that is:

$$\begin{aligned} &\boldsymbol{\Omega}\left[\boldsymbol{A}(\boldsymbol{X}_1, \boldsymbol{X}_2) + \boldsymbol{B}(\boldsymbol{X}_1, \boldsymbol{X}_2)(\boldsymbol{U_{eq}} + \boldsymbol{U_{sw}}) + \boldsymbol{L}(\boldsymbol{X}_1)\boldsymbol{F}_d\right] \\ &\qquad + \boldsymbol{\Phi}(\boldsymbol{X}_1, \boldsymbol{X}_2) = \begin{bmatrix} -K_1 s_x - \eta_1 \mathrm{sgn}(s_x) \\ 0 \\ -K_2 s_l - \eta_2 \mathrm{sgn}(s_l) \end{bmatrix} \end{aligned} \tag{14}$$

where $\mathbf{U_{sw}} = [F_{sw},\ 0,\ F_{lsw}]^{\mathrm{T}}$ represents the robust switching control quantity of the control system, with K_1, K_2, η_1 and η_2 all as normal numbers. Substituting Equations (5), (9) and (10) into Equation (11), the solution below can be obtained (15), as shown at the bottom of the page.

Thus, the control law of the sliding mode controller can be expressed as:

$$\begin{cases} F = F_w + f - \left[c_1\dot{x} + c_2\dot{\theta} - \dot{f}_1(t)\right]\left(M + m\sin^2\theta\right) \\ \quad + \dfrac{\cos\theta}{l}F_\theta \\ \quad -\dot{\theta}^2 lm\sin\theta + \left[c_3\dot{l} - \dot{f}_2(t)\right]msin\theta + gm\cos\theta\sin\theta \\ \quad + \left[-K_1 s_x - \eta_1 \mathrm{sgn}(s_x)\right]\left(M + m\sin^2\theta\right) \\ \quad -m\left[-K_2 s_l - \eta_2 \mathrm{sgn}(s_l)\right]\sin\theta \\ F_l = -m\left(l\dot{\theta}^2 + \left[c_3\dot{l} - \dot{f}_2(t)\right]\right. \\ \quad \left. - \left[c_1\dot{x} + c_2\dot{\theta} - \dot{f}_1(t)\right]\sin\theta + gl\sin\theta\right) \\ \quad +m\left(\left[-K_2 s_l - \eta_2 \mathrm{sgn}(s_l)\right] - \left[-K_1 s_x - \eta_1 \mathrm{sgn}(s_x)\right]\sin\theta\right) \end{cases} \tag{16}$$

Apparently, the sliding mode control law in Equation (16) demonstrates discontinuity, which will induce high frequency chattering of the output signal of the controller and will take

$$\begin{bmatrix} F_{eq} \\ F_{leq} \end{bmatrix} = \begin{bmatrix} F_w + f - \left[c_1\dot{x} + c_2\dot{\theta} - \dot{f}_1(t)\right]\left(M + m\sin^2\theta\right) + \dfrac{\cos\theta}{l}F_\theta \\ -\dot{\theta}^2 lm\sin\theta + \left[c_3\dot{l} - \dot{f}_2(t)\right]msin\theta + gm\cos\theta\sin\theta \\ -m\left(l\dot{\theta}^2 + \left[c_3\dot{l} - \dot{f}_2(t)\right] - \left[c_1\dot{x} + c_2\dot{\theta} - \dot{f}_1(t)\right]\sin\theta + gl\sin\theta\right) \end{bmatrix} \tag{12}$$

$$\boldsymbol{U_{sw}} = \begin{bmatrix} \left[-K_1 s_x - \eta_1 \mathrm{sgn}(s_x)\right]\left(M + m\sin^2\theta\right) - m\left[-K_2 s_l - \eta_2 \mathrm{sgn}(s_l)\right]\sin\theta \\ 0 \\ m\left(\left[-K_2 s_l - \eta_2 \mathrm{sgn}(s_l)\right] - \left[-K_1 s_x - \eta_1 \mathrm{sgn}(s_x)\right]\sin\theta\right) \end{bmatrix} \tag{15}$$

a toll on the actuator in practical engineering applications. The fact that the chattering phenomenon cannot be eliminated but only reduced by designing adaptive switching gain, filter, high-order sliding mode surface [28], [29] and other methods has prompted us to design a smooth and continuous switching function sat(*) in this paper to replace the symbolic function sgn(*) in the control law (13), which can reduce chattering and the complexity of controller structure. Equation (15) explains its specific definition.

$$sat(\mathbf{s}_i)\begin{cases} 1, & \mathbf{s}_i > \dfrac{\pi}{e^{\varepsilon}} \\ \sin(\dfrac{e^{\varepsilon}\mathbf{s}_i}{2}), & \dfrac{\pi}{e^{\varepsilon}} > \mathbf{s}_i > -\dfrac{\pi}{e^{\varepsilon}} \\ -1, & \mathbf{s}_i < -\dfrac{\pi}{e^{\varepsilon}} \end{cases} \tag{17}$$

where $\mathbf{s}_i = [s_x, s_l]^{\mathrm{T}}$. Next, a theorem will be incorporated to prove that the designed GESMC(see Equation (14)) satisfies asymptotic stability in the Lyapunov sense.

C. CONTROLLER STABILITY ANALYSIS

Theorem: For the two-dimensional bridge crane model described in Equation (5), with the adoption of the GESMC of Equation (11) to control the closed-loop control system and the controller parameters c_1, c_2, c_3, K_1, K_2, η_1, η_2, k_1 and k_2 kept more than 0, the closed-loop control system can be endowed with asymptotical stability.

Proof: If the closed-loop control system proposed is asymptotically stable, then the controller shall satisfy that the sliding variable $s(t)$ and its derivative $\dot{s}(t)$ can converge to the origin in certain period of time during the whole control process. Lyapunov energy functions for the whole sliding mode surface s_x and s_l are selected as follows:

$$V_x = \frac{1}{2}s_x^2 \tag{18}$$

$$V_l = \frac{1}{2}s_l^2 \tag{19}$$

Take the first-order derivative of Equations (18) and (19) with respect to time with its results showing in Equation (20) and (21).

$$\dot{V}_x = s_x\dot{s}_x \tag{20}$$

$$\dot{V}_l = s_l\dot{s}_l \tag{21}$$

Derived from Equation (9) of sliding mode dynamics with respect to time, the following equation can be obtained after simplification with substitution in Equation (20) and (21):

$$\begin{aligned}
&\dot{V}_x \\
&= s_x\boldsymbol{\lambda}_x\left[\boldsymbol{A}(\boldsymbol{X}_1,\boldsymbol{X}_2)+\boldsymbol{B}(\boldsymbol{X}_1,\boldsymbol{X}_2)\boldsymbol{U}+\boldsymbol{L}(\boldsymbol{X}_1)\boldsymbol{F}_d+\boldsymbol{\Phi}(\boldsymbol{X}_1,\boldsymbol{X}_2)\right] \\
&= s_x\Bigg[\frac{glm-glm\cos^2\theta+2\dot{\theta}^2lm\sin\theta}{M} \\
&\quad+\frac{F-f-F_w}{M}+\frac{\sin\theta F_l-gm\cos\theta\sin\theta}{M} \\
&\quad-\frac{\cos\theta F_\theta}{Ml}+c_1\dot{x}+c_2\dot{\theta}-\dot{f}_1(t)\Bigg]
\end{aligned} \tag{22}$$

$$\begin{aligned}
&\dot{V}_l \\
&= s_l\boldsymbol{\lambda}_l\left[\boldsymbol{A}(\boldsymbol{X}_1,\boldsymbol{X}_2)+\boldsymbol{B}(\boldsymbol{X}_1,\boldsymbol{X}_2)\boldsymbol{U}+\boldsymbol{L}(\boldsymbol{X}_1)\boldsymbol{F}_d+\boldsymbol{\Phi}(\boldsymbol{X}_1,\boldsymbol{X}_2)\right] \\
&= s_l\Bigg[\frac{2\dot{\theta}^2lm+gm\cos^3\theta+glm\sin\theta+M\dot{\theta}^2l}{M} \\
&\quad+\frac{-gm\cos\theta-2\dot{\theta}^2lm\cos^2\theta-glm\cos^2\theta\sin\theta}{M} \\
&\quad+\frac{M+m-m\cos^2\theta}{Mm}F_l+\frac{\sin\theta}{M}(F-f-F_w) \\
&\quad+gl\sin\theta-\frac{\cos\theta\sin\theta}{Ml}F_\theta+c_3\dot{l}-\dot{f}_2(t)\Bigg]
\end{aligned} \tag{23}$$

Substituting GESMC as shown in Equation (16) into Equation (22) and Equation (23), it can be obtained after simplification:

$$\dot{V}_x = -K_1s_x^2-\eta_1|s_x| \le 0 \tag{24}$$

$$\dot{V}_l = -K_2s_l^2-\eta_2|s_l| \le 0 \tag{25}$$

Equation (24) and (25) show that the input of the GESMC controller designed in this paper satisfies the generalized sliding mode condition: $\forall s_i \neq 0$, $\dot{V} = s_i\dot{s}_i < 0$. $\dot{V} = s_i\dot{s}_i = 0$ is true if and only if $\mathbf{s}_i = 0$ which means the sliding mode exists and each controlled quantity $e_i(i = x, \theta, l)$ deviation converges to zero simultaneously. With all these evidence, it can be verified that the proposed GESMC is asymptotically stable.

IV. SIMULATION ANALYSIS

In this section, a series of simulation experiments will be carried out in the MATLAB/Simulink environment to prove the potency and robustness of the proposed controller. In the simulation experiments, the physical parameters of the bridge crane system are set as follows:

$$M = 10\text{kg}, \quad m = 5\text{kg}, \quad l_0 = 2\text{m}, \quad \mu = 0.02, \quad k = 1,$$
$$s_1 = 0.002\text{m}^2, \quad s_2 = 0.004\text{m}^2, \quad \text{g} = 9.81\text{m/s}^2.$$

In the simulation process, the controller aims to ensure the crane to move from the initial position $x = 0$m to the target position $x_d = 1$m, while the wire rope l decreases from the initial state $l_0 = 2$m to $l_\text{d} = 1$m, and the swing angle of the payload comes at 0° at the end of the process.

For the purpose of better verifying the performance of the proposed GESMC, two methods of CSMC [30] and PID control are selected as comparison of the control effect in the two-dimensional bridge crane system with variable rope length. To ensure the integrity of the article, the expressions of the two controllers are given here.

A. CSMC CONTROLLER

$$\begin{aligned}
F = M\Bigg[&l-K_1s_x-\eta_1\mathrm{sgn}(s_x)-c_1\dot{x}-c_2\dot{\theta} \\
&+\frac{1}{M}(f+F_w)+\frac{\cos\theta}{Ml}F_\theta-\frac{\sin\theta}{M}F \\
&-\frac{glm-glm\cos^2\theta+2\dot{\theta}^2lm\sin\theta-gm\cos\theta\sin\theta}{M}\Bigg]
\end{aligned}$$

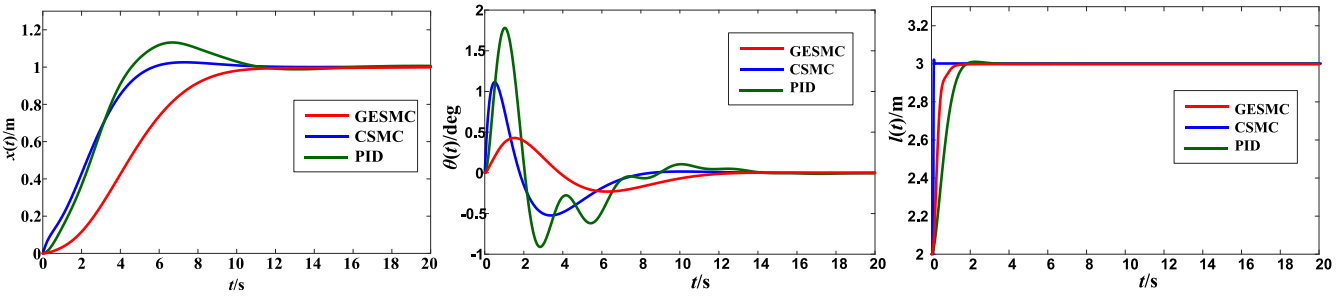

(a) Crane position (b) Payload swing Angle (c) Wire rope length

FIGURE 2. The comparative experiment of three control methods.

$$F_l = \frac{Mm}{M+m-m\cos^2\theta} \times \left[-K_2 s_l - \eta_2 \mathrm{sgn}(s_l) - c_3\dot{l} - \frac{sin\theta}{M}F + \frac{sin\theta}{M}(f+F_w) + \frac{cos\theta sin\theta}{Ml}F_\theta - \frac{2\dot{\theta}^2 lm\cos^2\theta}{M} + \frac{2\dot{\theta}^2 lm + gm\cos^3\theta + Mgl\sin\theta - glm\cos^2\theta\sin\theta}{M} + \frac{glm\sin\theta + M\dot{\theta}^2 l - gm\cos\theta}{M}\right]$$

where c_1, c_2 and $c_3 \in \mathbb{R}^+$ denote the sliding constants, η_1, η_2, K_1, and $K_2 \in \mathbb{R}^+$ are the SMC gains. Moreover, $s_x(t)$ and $s_x(t)$ represent the position sliding mode surface and the lifting sliding mode surface respectively, which are defined as follows:

$$s_x(t) = \dot{x} + c_1(x - x_d) + c_2\theta$$
$$s_l(t) = \dot{l} + c_3(l - l_d)$$

B. PID CONTROLLER

$$F = k_{1\mathrm{p}}(x - x_d) + k_{1\mathrm{i}}\int_0^t (x - x_d)d\tau + k_{1\mathrm{d}}\dot{x} - k_{2\mathrm{p}}\theta - k_{2\mathrm{i}}\int_0^t \theta d\tau - k_{2\mathrm{d}}\dot{\theta}$$
$$F_l = k_{3\mathrm{p}}(l - l_d) + k_{3\mathrm{d}}\dot{l}$$

where $k_{1\mathrm{p}}$, $k_{2\mathrm{p}}$, $k_{3\mathrm{p}}$, $k_{1\mathrm{i}}$, $k_{2\mathrm{i}}$, $k_{1\mathrm{d}}$, $k_{2\mathrm{d}}$ and $k_{3\mathrm{d}} \in \mathbb{R}^+$ and all control gains.

In order to solve the optimal parameter selection problem caused by the complex structure of GESMC method, this paper uses Cuckoo Search Algorithm with Adaptively Selecting Crossover Points (ASCP-CS) method [30] to set its parameters. To avoid loss of generality, the same optimization method is used to solve the parameter selection problem of the two comparison methods. After a large number of optimization experiments, the parameters of three controllers are adjusted as the Table 2 showed:

Arrangement of Experiments: The following four groups of simulation experiments based on different working conditions are designed to prove respectively the control performance of GESMC and its robustness to cope with common conditions such as external disturbance, payload and damping changes in engineering applications:

TABLE 2. Control gains.

Controllers	Control gains
GESMC controller	c_1=0.6, c_2=5, c_3=100, η_1=0.1, η_2=1, K_1=36, K_2=50, k_1=50, k_2=41
CSMC controller	c_1=0.4, c_2=20, c_3=80, η_1=0.6, η_2=0.1, K_1=100, K_2=70
PID controller	$k_{1\mathrm{p}}$=5, $k_{2\mathrm{p}}$=6, $k_{3\mathrm{p}}$=30, $k_{1\mathrm{i}}$=0.01, $k_{2\mathrm{i}}$=1, $k_{1\mathrm{d}}$=10, $k_{2\mathrm{d}}$=12, $k_{3\mathrm{d}}$=20

1) SIMULATION GROUP 1

Under accurate parameters and no external interference, this paper adopts GESMC to carry out anti-swing positioning control for the two-dimensional bridge crane system, whose data is presented in Figure 2-3.

Figure 2 presents the performance curves of the three controllers with determined model parameters and no external interference. Conclusions from the comparative analysis: a) The crane position, payload swing Angle and wire rope length reach the target state within 12s, 14s and 3s respectively. b) Compared with PID controller, two sliding mode controllers require longer crane operating positioning time but possess less crane position overshooting, payload swing and frequency, and higher speed of wire rope length reaching the target position. c) The performance comparison of the two sliding mode controllers conveys that the GESMC designed in this paper features with smaller payload swing and frequency within 11s of the crane adjustment time, and no obvious overshot phenomenon has been observed at the crane position and the rope length of the steel wire.

Fig. 3(a) and (c) show the change curve of system control quantity F and F_l using GESMC, while Fig. 3(b) and (d) present the change curve of system control quantity F and F_l using the sliding mode controller based on the reaching law. Conclusions from the analysis of Figure 3: a) Since the initial control quantity of GESMC is much smaller than that of the approach law sliding mode controller,

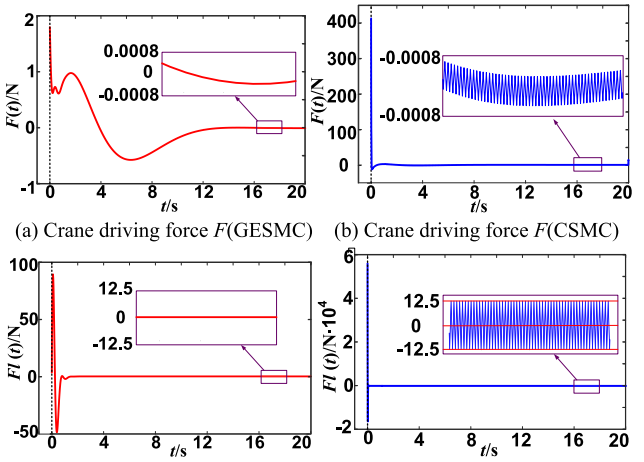

(a) Crane driving force F(GESMC) (b) Crane driving force F(CSMC)

(c)Wire rope lifting force F_l(GESMC)(d)Wire rope lifting force F_l(CSMC)

FIGURE 3. The change of system control quantity F and Fl of two sliding mode controllers.

the designed controller can reduce the requirement on the maximum output torque of the executive motor. b) Thanks to the effective suppression of the chattering phenomenon in GESMC, the damage to the actuating motor can be undermined considerably, which favorably promotes its engineering application.

Based on the simulation analysis above, GESMC stands better control effect compared with CSMC and PID control.

2) SIMULATION GROUP 2

Multi-group simulation experiments are conducted with most of the system parameter settings in simulation case 1 remaining the same but the payload mass. Then, it is compared and analyzed with the control effect of CSMC method. In these experiments, the mass of the payload is 5kg, 15kg and 30kg respectively.

Fig. 4(a), (b) and (c) refer to the variation curves of various state quantities of the bridge crane system under the control of GESMC and under different payload mass conditions. Fig. 4(d), (e) and (f) provide the variation curve of system output after the sliding mode controller based on the reaching law is adopted in the bridge crane system under different payload mass conditions. From the local zoomed Fig. 4(a) and (b), when the controller control gain stays the same in the case of GESMC, changing payload mass casts minimal influence on the crane position and payload swing angle control performance, and it can be basically overlooked. In contrast, although low sensitivity shows up in the approach law sliding mode controller during payload mass changes, significant fluctuation can still be observed in the control performance curves of the three payload mass conditions, indicating that the approach law sliding mode controller is defeated by GESMC in robustness during payload mass changes. Further analysis shows that the mass and the overshoot of the two controllers in the aspect of rope length are positively correlated and overshoot of the GESMC controller designed in this paper is lower than that of the sliding mode controller with the approach law.

3) SIMULATION GROUP 3

This group describes the changes of control effect of equivalent sliding mode controller in the whole process under different air resistance and track friction conditions:

Working Condition 1: The friction coefficient between the crane and the track remains constant at $\mu = 0.02$ and the air damping coefficient is adopted at $k = 1, 5$ and 10 to carry out the simulation experiment, whose results are listed in figure 5.

Fig. 5 tells that the performance curve of the designed GESMC only changes mildly when the air resistance coefficient k is changed. Specifically, with the increase of the air resistance coefficient k, the crane positioning running time and the time for the payload to drops to the specified height increase by though less than 0.001 shown in Fig. 5(a) and (b). The increase of payload swing can also be controlled below 0.001°, as shown in the local zoomed figure in Figure 5(c), which can basically be regarded as having no effect on the controller performance.

Working Condition 2: The air damping coefficient remains constant at $k = 1$ and the friction coefficient is adopted at $\mu = 0.02$, 0.2 and 1 between the crane and the track to carry out the simulation experiment, whose results are shown in Figure 6.

As for the change of friction coefficient, the sensitivity of the system is even lower. By observing Figure 6(a)-(c), we can see that the control performance curves of the system under the three friction coefficients basically superimpose.

After the analysis above, a conclusion can be drawn that when the payload mass, damping force and friction coefficient between the crane and the track change, or there are uncertain factors, the GESMC displays less sensitivity to the change of model parameters but has strong robustness.

4) SIMULATION GROUP 4

Based on the settings in simulation group 1, rectangular wave interference signals with a duration of 0.5s and a relative amplitude of 15% are applied to the payload swing angle at $t = 12$s to simulate man-made or natural disturbances (such as strong wind and obstacle obstruction) encountered unexpectedly during the operation of the system. The experimental results are shown in Fig. 7.

Influence of rectangular wave interference on crane displacement $x(t)$ and wire rope length $l(t)$: seen from Fig. 7(a) and (c), the transient and steady-state responses of the three controllers in the case of crane displacement $x(t)$ and wire rope length $l(t)$ stay almost unaffected and bear good control performance. The comparison is clearly illustrated by Fig. 2(a) and (c).

Influence of rectangular wave interference on payload swing angle $\theta(t)$: Fig. 7(b) shows that: a) In terms of payload swing angle $\theta(t)$ control, all three controllers sway around the equilibrium point to varying degrees under the action of rectangular wave disturbance signals, but all converge to zero

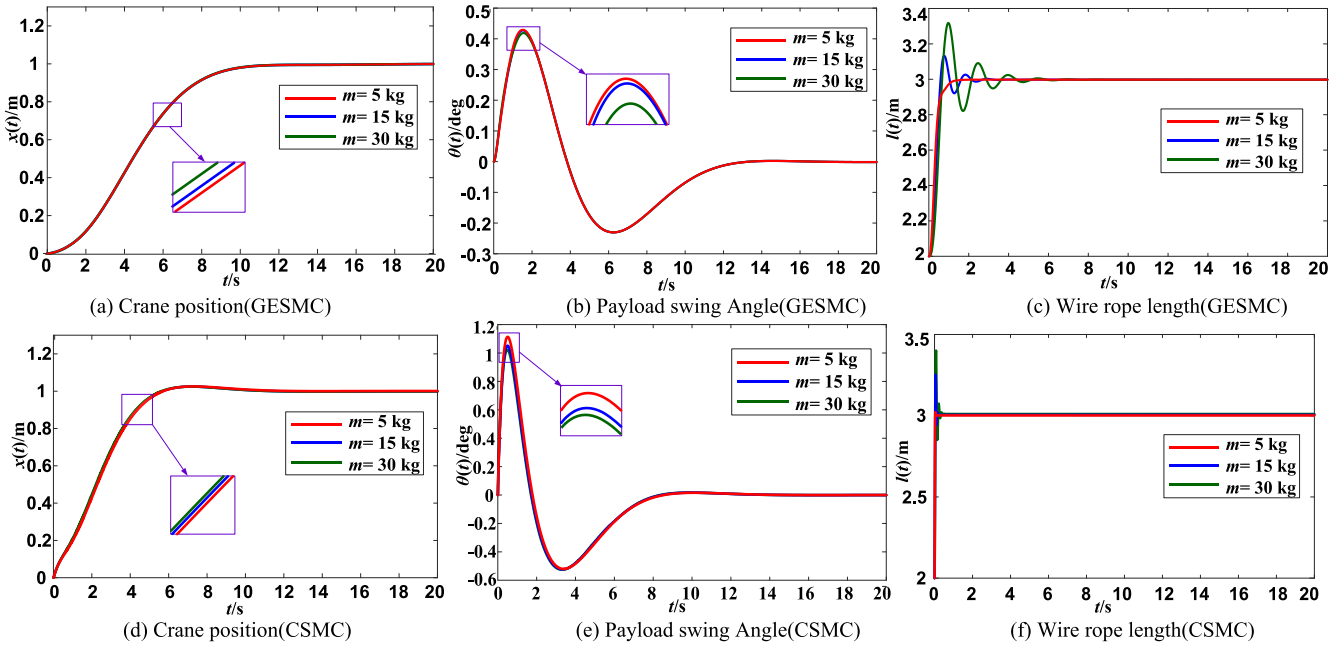

(a) Crane position(GESMC) (b) Payload swing Angle(GESMC) (c) Wire rope length(GESMC)

(d) Crane position(CSMC) (e) Payload swing Angle(CSMC) (f) Wire rope length(CSMC)

FIGURE 4. Control effect of the two control algorithms changes when the payload quality changes.

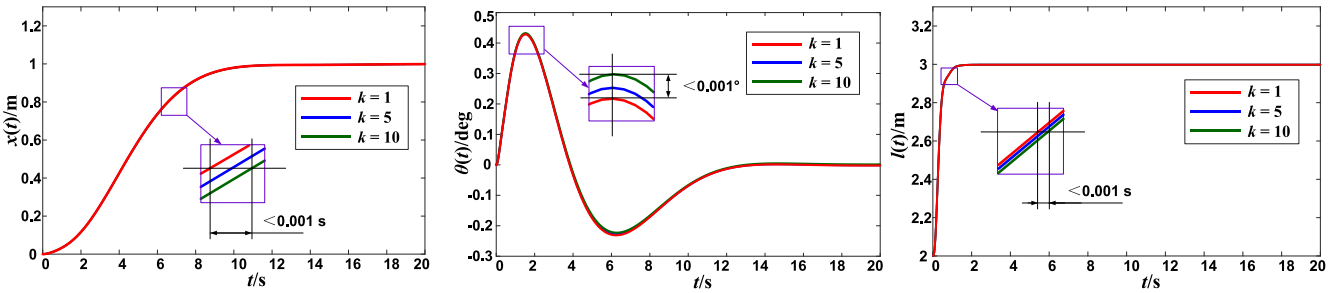

(a) Crane position (b) Payload swing Angle (c) Wire rope length

FIGURE 5. Global-equivalent sliding mode control effect under different air resistance(μ=0.02).

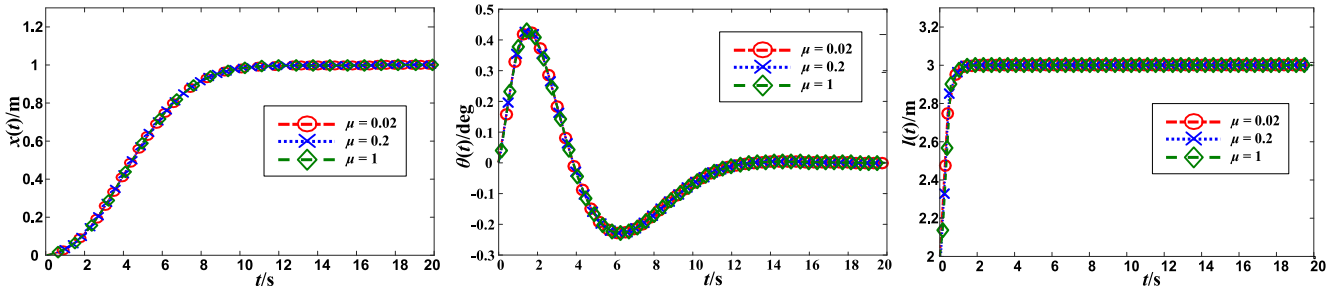

(a) Crane position (b) Payload swing Angle (c) Wire rope length

FIGURE 6. Global-equivalent sliding mode control under different friction force.

within 3.5s after the end of disturbance. b) Further observation shows that the GESMC can quickly adjust the motion of the crane within 0.18s after the end of interference, and effectively eliminate the remaining swing angle caused by external interference. However, CSMC method restores the stability of payload swing angle after 0.21s adjustment, while the PID controller needs about 1s to realize payload stabilization control, as shown in the partial enlarged view in Fig.7(b). c) When subjected to external disturbance, the sliding mode controller has better robustness than the PID controller. It is

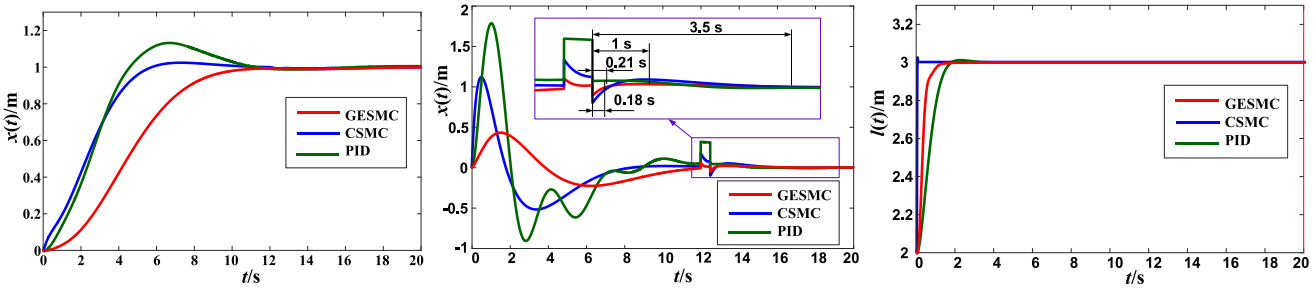

(a) Crane position (b) Payload swing Angle (c) Wire rope length

FIGURE 7. Variation curves of crane displacement, wire rope length and payload swing angle.

worth noting that, when the interference signal is applied, two sliding mode controllers are in the sliding mode approaching stage, and the proposed controller can eliminate the residual swing faster than CSMC does, which indicates strong robustness in the sliding mode approaching stage and global robustness of the proposed controller.

In summary, through four groups of simulation and comparison experiments, it is verified that GESMC has better transient and steady state responses than PID controller and CSMC do, and it is less sensitive to changes of model parameters (including load mass, air resistance coefficient and friction coefficient), and has strong robustness to external disturbances and global robustness.

V. CONCLUSION

In order to realize the global robust control of the bridge crane system, this paper proposes a new sliding mode control method which incorporates global sliding mode manifold with equivalent sliding mode control for bridge crane system. Different from the current traditional sliding mode control, this controller introduces a whole sliding mode surface with global robustness, so as to keep the system in the sliding mode dynamic stage from the initial state, which can improve the robustness of the system. Moreover, regarding to the severe output chattering problem, a saturation function is designed to replace the switching function. By setting four groups of simulation experiments under different working conditions, the proposed controller presents the better transient and steady state responses than the CSMC and the PID controllers do and also, and possesses low output chattering effect. Friction and air resistance almost pose no effect in responding to the variable payload mass and the proposed controller can efficiently achieve the elimination of residual swing effect, displaying a high robustness. Inspired by the existing work, the proposed controller will be tested on the platform of crane experiment hardware in the follow-up research to further verify its predominant performance.

REFERENCES

[1] H. Rams, M. Schöberl, and K. Schlacher, "Optimal motion planning and energy-based control of a single mast stacker crane," *IEEE Trans. Control Syst. Technol.*, vol. 26, no. 4, pp. 1449–1457, Jul. 2018.

[2] D. Wang, H. He, and D. Liu, "Intelligent optimal control with critic learning for a nonlinear overhead crane system," *IEEE Trans. Ind. Informat.*, vol. 14, no. 7, pp. 2932–2940, Jul. 2018.

[3] N. Sun, J. Zhang, X. Xin, T. Yang, and Y. Fang, "Nonlinear output feedback control of flexible rope crane systems with state constraints," *IEEE Access*, vol. 7, pp. 136193–136202, 2019.

[4] M. Zhang, Y. Zhang, and X. Chen, "Finite-time trajectory tracking control for overhead crane systems subject to unknown disturbances," *IEEE Access*, vol. 7, pp. 55974–55982, 2019.

[5] G. Peláez, J. Vaugan, P. Izquierdo, H. Rubio, and J. C. García-Prada, "Dynamics and embedded Internet of Things input shaping control for overhead cranes transporting multibody paypayloads," *Sensors*, vol. 18, no. 6, pp. 17–18, Jun. 2018.

[6] X. Xie, J. Huang, and Z. Liang, "Vibration reduction for flexible systems by command smoothing," *Mech. Syst. Signal Process.*, vol. 39, nos. 1–2, pp. 461–470, Aug. 2013.

[7] P. A. Ospina-Henao and F. López-Suspes, "Dynamic analysis and control PID path of a model type gantry crane," *J. Phys., Conf. Ser.*, vol. 850, no. 1, pp. 1–14, Jun. 2017.

[8] L. Xiao, W. Li, W. Wang, and Z. Xu, "Control for the new harsh sea conditions salvage crane based on modified fuzzy PID," *Asian J. Control*, vol. 20, no. 2, pp. 1582–1594, Jul. 2018.

[9] X. Lai, Y. Liu, Y. Dai, and W. Luo, "Adaptive neural network control and learning of bridge crane system," *Mech. Des. Manuf.*, vol. 6, pp. 114–117, Jun. 2018.

[10] L. A. Tuan and S.-G. Lee, "Sliding mode controls of double-pendulum crane systems," *J. Mech. Sci. Technol.*, vol. 27, no. 6, pp. 1863–1873, Jul. 2013.

[11] E. Q. Hussein, A. Q. Al-Dujaili, and A. R. Ajel, "Design of sliding mode control for overhead crane systems," in *Proc. IOP Conf. Ser. Mater. Sci. Eng.*, vol. 881. Jun. 2020, Art. no. 012084.

[12] D. Qian and J. Yi, *Overhead Crane Control by Hierarchical Sliding Mode*. Berlin, Germany: Springer, 2016, pp. 117–166.

[13] B. Liu, W. Xu, J. Chu, and X. Zhou, "Multi-sliding mode structure control of bridge crane," *Control Eng.*, vol. 19, no. 1, pp. 78–80, Jan. 2012.

[14] H. Ouyang, J. Wang, G. Zhang, L. Mei, and X. Deng, "Novel adaptive hierarchical sliding mode control for trajectory tracking and load sway rejection in double-pendulum overhead cranes," *IEEE Access*, vol. 7, pp. 10353–10361, 2019.

[15] C. Zhang, Z. Lin, S. X. Yang, and J. He, "Total-amount synchronous control based on terminal sliding-mode control," *IEEE Access*, vol. 5, pp. 5436–5444, 2017.

[16] B. Xu, L. Zhang, and W. Ji, "Improved non-singular fast terminal sliding mode control with disturbance observer for PMSM drives," *IEEE Trans. Transport. Electrific.*, early access, May 26, 2021, doi: 10.1109/TTE.2021.3083925.

[17] Y. Wang and W. Xu, "Synchronous control of double-container overhead crane based on PI terminal sliding mode," *Int. Core J. Eng.*, vol. 6, no. 5, pp. 133–143, May 2020.

[18] T. Yu, H. Sun, Q. Jia, Y. Zhang, and W. Zhao, "Decoupling sliding mode control method for a class of underactuated systems," *J. Southeast Univ.*, vol. 42, no. 1, pp. 11–14, Jun. 2012.

[19] Y. Tao, Y. Kun, and Z. Wei, "Anti-swing control of bridge crane system based on decoupling sliding mode control," *China Test*, vol. 43, no. 8, pp. 95–100, Aug. 2017.

[20] L. A. Tuan, S.-G. Lee, L. C. Nho, and D. H. Kim, "Model reference adaptive sliding mode control for three dimensional overhead cranes," *Int. J. Precis. Eng. Manuf.*, vol. 14, no. 8, pp. 1329–1338, Aug. 2013.
[21] M. Zhang, X. Ma, R. Song, X. Rong, G. Tian, X. Tian, and Y. Li, "Adaptive proportional-derivative sliding mode control law with improved transient performance for underactuated overhead crane systems," *IEEE/CAA J. Autom. Sin.*, vol. 5, no. 3, pp. 683–690, May 2018.
[22] G.-H. Kim and K.-S. Hong, "Adaptive sliding-mode control of an offshore container crane with unknown disturbances," *IEEE/ASME Trans. Mechatronics*, vol. 24, no. 6, pp. 2850–2861, Dec. 2019.
[23] Y. Xue, B.-C. Zheng, and X. Yu, "Robust sliding mode control for T-S fuzzy systems via quantized state feedback," *IEEE Trans. Fuzzy Syst.*, vol. 26, no. 4, pp. 2261–2272, Aug. 2018.
[24] S. Pezeshki, M. A. Badamchizadeh, A. R. Ghiasi, and S. Ghaemi, "Control of overhead crane system using adaptive model-free and adaptive fuzzy sliding mode controllers," *J. Control, Autom. Electr. Syst.*, vol. 26, no. 1, pp. 1–15, Feb. 2015.
[25] T. Mizoshiri and Y. Mori, "Sliding mode control with a time-varying ellipsoidal sliding surface," in *Proc. IEEE/SICE Int. Symp. Syst. Integr. (SII)*, Paris, France, Jan. 2019, pp. 165–170.
[26] Y. Cui and L. Xu, "Chattering-free adaptive sliding mode control for continuous-time systems with time-varying delay and process disturbance," *Int. J. Robust Nonlinear Control*, vol. 29, no. 11, pp. 3389–3404, Apr. 2019.
[27] Y.-S. Lu, C.-W. Chiu, and J.-S. Chen, "Time-varying sliding-mode control for finite-time convergence," *Electr. Eng.*, vol. 92, nos. 7–8, pp. 257–268, Dec. 2010.
[28] Q. Hou and S. Ding, "GPIO based super-twisting sliding mode control for PMSM," *IEEE Trans. Circuits Syst. II, Exp. Briefs*, vol. 68, no. 2, pp. 747–751, Feb. 2021.
[29] Q. Hou, S. Ding, and X. Yu, "Composite super-twisting sliding mode control design for PMSM speed regulation problem based on a novel disturbance observer," *IEEE Trans. Energy Convers.*, early access, Apr. 6, 2020, doi: 10.1109/TEC.2020.2985054.
[30] T. Wang, N. Tan, X. Zhang, G. Li, S. Su, J. Zhou, J. Qiu, Z. Wu, Y. Zhai, R. D. Labati, V. Piuri, and F. Scotti, "A time-varying sliding mode control method for distributed-mass double pendulum bridge crane with variable parameters," *IEEE Access*, vol. 9, pp. 75981–75992, 2021.
[31] T. Wang, N. Tan, R. Zhang, J. Qiu, and K.-T. Kin, "Design of a sliding mode controller of bridge crane based on ASCP-CS algorithm," *J. Hunan Univ.*, vol. 47, no. 6, pp. 87–95, Jun. 2020.

TIANLEI WANG (Member, IEEE) received the B.S.E. degree in electrical engineering from Beijing University of Posts and Telecommunications, and the M.S. degree in signal processing from the South China University of Technology. He is currently pursuing the Ph.D. degree with Beijing Jiaotong University. His research interests include the intelligent systems, control theory, and pattern recognition.

NANLIN TAN is currently a Professor and a Ph.D. Supervisor of Beijing Jiaotong University, Beijing, China. His current research interests include safety technology engineering, control theory, and pattern recognition.

JIONGZHI QIU was born in Lufeng, Guangdong, China, in December 1999. He is currently pursuing the bachelor's degree in traffic engineering with the Intelligent Manufacturing Division, Wuyi University. His main research interests include underdrive system modeling and nonlinear control.

YANJIANG YU received the bachelor's degree from Wuyi University. He is currently pursuing the master's degree majoring in mechanical manufacturing and automation with the School of Mechanical and Automotive Engineering, South China University of Technology. His research interests include signal processing and optimization algorithm.

XIANWEN ZHANG was born in Qingyuan, Guangdong, China, in December 1997. He is currently pursuing the bachelor's degree in traffic engineering with the Intelligent Manufacturing Division, Wuyi University. His main research interests include underdrive system modeling and nonlinear control.

YIKUI ZHAI (Member, IEEE) received the bachelor's and master's degrees in optical electronics information and communication engineering, and signal and information processing from Shantou University, Guangdong, China, in 2004 and 2007, respectively, and the Ph.D. degree in signal and information processing from Beihang University, in June 2013. Since October 2007, he has been working with the Department of Intelligence Manufacturing, Wuyi University, Guangdong. He was a Visiting Scholar with the Department of Computer Science, University of Milan, from June 2016 to June 2017. He is currently an Associate Professor with Wuyi University. His research interests include image processing, biometric extraction, deep learning, and pattern recognition.

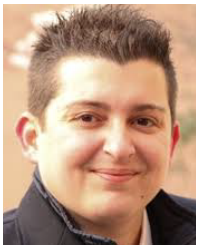

RUGGERO DONIDA LABATI (Member, IEEE) received the Ph.D. degree in computer science from the Universitá degli Studi di Milano, Crema, Italy, in 2013. He has been an Assistant Professor in computer science with the Universitá degli Studi di Milano, since 2015. He has also been a Visiting Researcher with Michigan State University, East Lansing, MI, USA. Original results have been published in more than 50 papers in international journals, proceedings of international conferences, books, and book chapters. His current research interests include intelligent systems, signal and image processing, machine learning, pattern analysis and recognition, theory and industrial applications of neural networks, biometrics, and industrial applications. He is an Associate Editor of the *Journal of Ambient Intelligence and Humanized Computing* (Springer).

VINCENZO PIURI (Fellow, IEEE) received the M.S. and Ph.D. degrees in computer engineering from the Politecnico di Milano, Italy. He was an Associate Professor with the Politecnico di Milano, from 1992 to 2000, and a Visiting Professor with The University of Texas at Austin, USA, from 1996 to 1999. He has been a Full Professor with the University of Milan, Italy, since 2000, where he was the Department Chair, from 2007 to 2012. He founded a start-up company, Sensure srl, in the area of intelligent systems for industrial applications leading it, from 2007 to 2010, and was active in industrial research projects with several companies. He was a Visiting Researcher with George Mason University, USA, from 2012 to 2016. His main research and industrial application interests include intelligent systems, computational intelligence, pattern analysis and recognition, machine learning, signal and image processing, biometrics, intelligent measurement systems, industrial applications, distributed processing systems, the Internet of Things, cloud computing, fault tolerance, application-specific digital processing architectures, and arithmetic architectures. He is an ACM Fellow.

FABIO SCOTTI (Senior Member, IEEE) received the Ph.D. degree in computer engineering from the Politecnico di Milano, Milan, Italy, in 2003. He has been an Associate Professor in computer science with the Universitá degli Studi di Milano, Crema, Italy, since 2015. Original results have been published in more than 100 papers in international journals, proceedings of international conferences, books, book chapters, and patents. His current research interests include biometric systems, machine learning and computational intelligence, signal and image processing, theory and applications of neural networks, three-dimensional reconstruction, industrial applications, intelligent measurement systems, and high-level system design. He is an Associate Editor of the IEEE TRANSACTIONS ON HUMAN-MACHINE SYSTEMS and *Soft Computing* (Springer).